JOURNAL OF MATERIALS SCIENCE 25 (1990) 5166–5172

Magnetic properties and surface crystallization induced by selective oxidation in Fe–B–Si amorphous alloy

N. MORITO, T. SUZUKI, C. MAEDA, T. YAMASHITA, Y. KITANO
Technical Research Division, Kawasaki Steel Corporation, Kawasaki-cho, Chiba 260, Japan

The relationship between the annealing atmosphere and the magnetic properties of $Fe_{78.5}B_{13}Si_{8.5}$ amorphous alloy has been studied, showing that annealing in nitrogen, argon, hydrogen and air significantly improved the iron loss of the amorphous ribbon, giving much better results than annealing in an $H_2 + H_2O$ atmosphere. A boron-depletion zone with the alloy composition 0 to 3 mol% B and 9 to 11 mol% Si was detected by Auger electron spectroscopy under the oxide film formed during annealing in $H_2 + H_2O$. The iron crystalline phase is formed only on the ribbon surface after annealing in $H_2 + H_2O$. A mechanism is proposed explaining the deleterious effect of annealing in the $H_2 + H_2O$, whereby the H_2O in this atmosphere selectively oxides boron in the amorphous alloy to form a B_2O_3 film and the boron-depletion zone, and the alloy in this zone is then crystallized into α-Fe. This surface crystalline layer induces out-of-plane magnetic anisotropy in the amorphous alloy ribbon (which was observed by transmission Mössbauer spectroscopy) and thus deterioration of the iron loss.

1. Introduction

The development of excellent soft magnetic properties in iron-base amorphous alloy ribbons requires annealing below the crystallization temperature and cooling in a magnetic field. The annealing treatment relieves the stress resulting from the casting operation, and cooling in the magnetic field induces a uniaxial anisotropy in the ribbon plane.

To obtain low iron losses and low excitation, annealing must be performed at a temperature high enough to relieve the residual stresses, but not so high as to cause crystallization of the amorphous alloy [1]. Ok and Morrish [2] reported that in annealed $Fe_{82}B_{12}Si_6$ amorphous ribbon an out-of-plane anisotropy developed as a consequence of surface crystallization, which preceded bulk crystallization.

In many cases, annealing is performed in an inert gas atmosphere or vacuum, in order to avoid the surface oxidation of the amorphous alloy. On the other hand, it has been reported that boron depletion at the surface occurs during annealing of Fe–B amorphous alloy in static and dynamic vacuums and causes surface crystallization [3, 4].

Köster [5] studied the influence of surface treatments or annealing atmosphere on surface crystallization behaviour of $Co_{72}Si_2B_{26}$ and $Fe_{39}Ni_{39}B_{22}$ amorphous ribbons and stressed the importance of local changes in surface composition by selective oxidation or segregation. However, no direct evidence of such local changes in composition at the amorphous ribbon surfaces was found.

The purpose of this study was to investigate the effect of various annealing atmospheres such as nitrogen, argon, oxygen hydrogen and $H_2 + H_2O$ gases on the behaviour of boron in the surface layer, surface crystallization, and the magnetic properties of $Fe_{78.5}B_{13}Si_{8.5}$ amorphous alloy ribbon.

2. Experimental procedure

An amorphous alloy with a nominal composition of $Fe_{78.5}B_{13}Si_{8.5}$ (mol %) was prepared by rapid quenching from the melt. The resulting ribbon was 50 mm wide and approximately 21×10^{-3} mm thick. The Curie temperature and the crystallization temperature were 683 and 803 K, respectively.

The magnetic properties were measured in a single sheet of the ribbon 150 mm long, which was previously annealed in a gas flowing atmosphere at temperatures between 623 and 698 K. For structural investigations, small ribbon pieces were cut from the samples for magnetic measurements.

Fourier transformation–infrared reflection spectroscopy (FT–IR) with an incident angle of 80° and electron spectroscopy for chemical analysis (ESCA) with an X-ray source of Al$K\alpha$ were used to identify oxide films and metallic phases at the ribbon surfaces after annealing in various annealing atmospheres.

Thin-film X-ray diffraction (XRD) with Cu$K\alpha$ ray at the fixed incident angle of 2° (Seemann-Bohlin geometry) was employed to identify thin surface crystalline phases formed during annealing. The $\sin^2\phi$ method was used in order to evaluate the residual stress in the surface crystalline layers.

Auger electron spectroscopy (AES) with a sputtering system using argon ions was used to study the composition profiles in a surface layer of annealed

0022–2461/90 $03.00 + .12

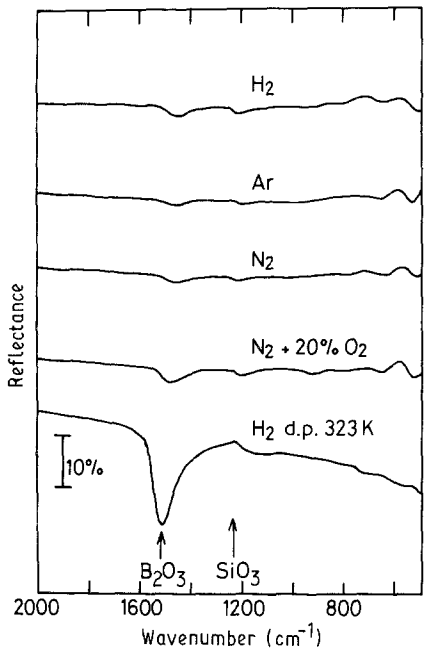

Figure 1 Infrared reflection spectra from $Fe_{78.5}B_{13}Si_{8.5}$ amorphous alloy annealed at 673 K for 3.6 ksec in various annealing atmospheres. d.p. = dew point.

ribbons. The sputtering rate of an iron plate by the argon ions was approximately 0.04 nm sec^{-1} under the conditions used here.

Conversion-electron emission and γ-ray absorption Mössbauer spectroscopy with ^{57}Co of about 20 mCi (1 Ci = 3.7 × 10^{10} Bq) were used to identify surface crystalline phases and to study the magnetic anisotropy in the amorphous ribbon bulk. The measurements were made at room temperature and α-Fe was used for the correction of speed.

3. Results and discussion

3.1. Surface oxidation

Infrared reflection spectra (Fig. 1) from Fe–B–Si amorphous alloy ribbons annealed at 673 K for 3.6 ksec

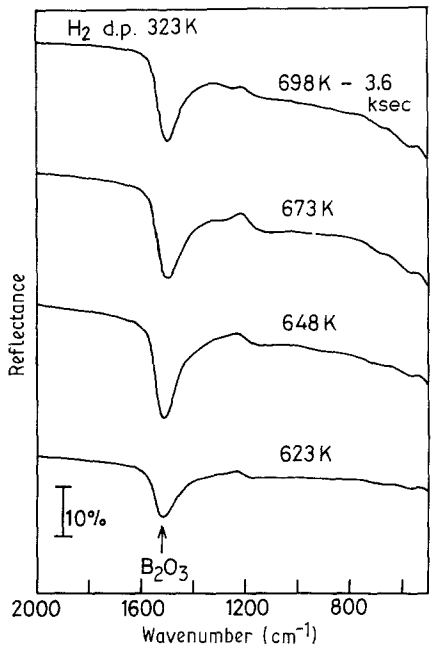

Figure 2 Change in infrared reflection spectra from $Fe_{78.5}B_{13}Si_{8.5}$ amorphous alloy annealed for 3.6 ksec in hydrogen with a dew point of 323 K upon annealing at various temperatures.

show that annealing in argon, nitrogen, dry hydrogen and N_2 + 20% O_2 atmospheres causes the formation of extremely thin oxide films of SiO_2 and B_2O_3. On the other hand, during annealing in hydrogen with a dew point of 323 K, a thick oxide film of B_2O_3 is formed.

The annealing temperature dependence of infrared reflection spectra from Fe–B–Si amorphous alloy ribbons annealed in hydrogen with a dew point of 323 K is shown in Fig. 2. The intensity of the absorption peak assigned to B_2O_3, i.e. the formation rate of B_2O_3 film on the ribbon surface, decreases with decreasing ânnealing temperature.

ESCA spectra (Fig. 3) show that iron and boron in the surface layer of Fe–B–Si amorphous alloy ribbons annealed at 673 K in a dry hydrogen atmosphere are mainly in the metallic states, and that only silicon is oxidized to form SiO_2 film. Annealing in hydrogen with a dew point of 323 K oxidizes silicon, iron and boron to form SiO_2, Fe_2O_3 and B_2O_3, respectively, on the ribbon surface. During annealing in an oxygen-containing nitrogen atmosphere, SiO_2 and B_2O_3 are formed on the amorphous alloy surface, but a small part of the iron in the surface layer remains in the metallic state.

These experimental results indicate that the water in the annealing atmosphere is more corrosive to Fe–B–Si amorphous ribbons than the oxygen, and that B_2O_3 film is less protective than SiO_2 film.

3.2. Depth profiles in the surface layer

The thick oxide films are formed at the surface of Fe–B–Si amorphous alloy ribbons annealed in a wet hydrogen atmosphere, as shown in infrared reflection spectra and ESCA analysis. Fig. 4 shows depth profiles of iron, boron, silicon and oxygen in the surface layer of Fe–B–Si amorphous alloy ribbons annealed at 673 K for 3.6 ksec in dry hydrogen and in hydrogen with a dew point of 323 K. In the ribbons annealed in dry hydrogen, silicon segregation was observed in the thin surface oxide film. The depth profiles of iron, boron and silicon in the alloy beneath the oxide film were almost flat and their concentrations were the same as the nominal alloy composition. These tendencies were also observed in the ribbons annealed in nitrogen and N_2 + 20% O_2 atmospheres.

On the other hand, the amorphous ribbon annealed in wet hydrogen had a thick oxide film with a remarkably high concentration of boron and silicon. Further, below the oxide layer a boron-depletion zone with a composition of 0 to 3 mol % B and 9 to 11 mol % Si was observed over a thickness of several tens of nanometres.

Fig. 5 shows the influence of annealing temperature on the thicknesses of the oxide films and the boron-depletion zones formed during annealing in a hydrogen atmosphere with a dew point of 323 K. The thickness of an oxide film formed on annealing at 623 K for 3.6 ksec is smaller than that after annealing at temperatures higher than 623 K, and it is approximately constant over the annealing temperature range 648 to 698 K. On the contrary, the thickness of the boron-depletion zones decreases with decreasing annealing temperature. The thickness of the boron-depletion

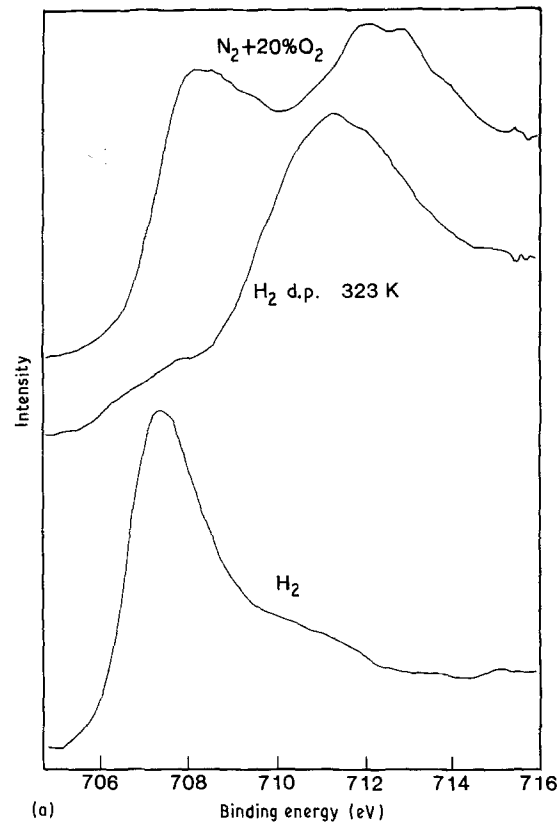

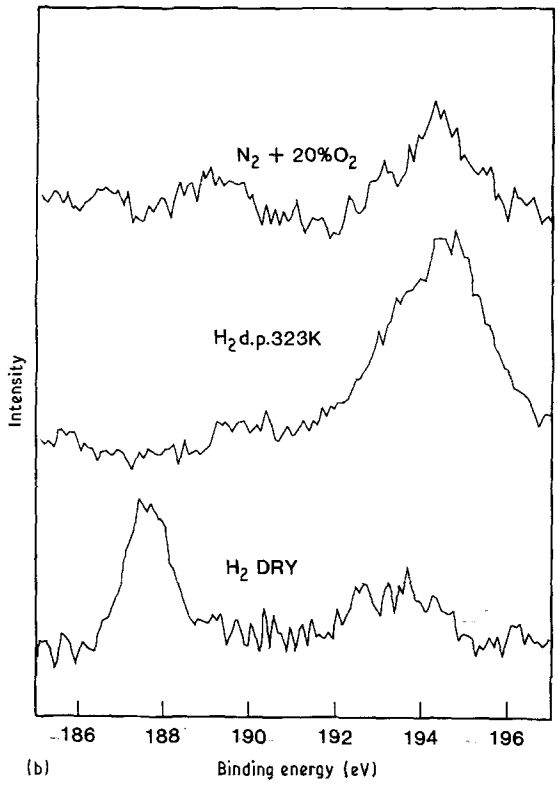

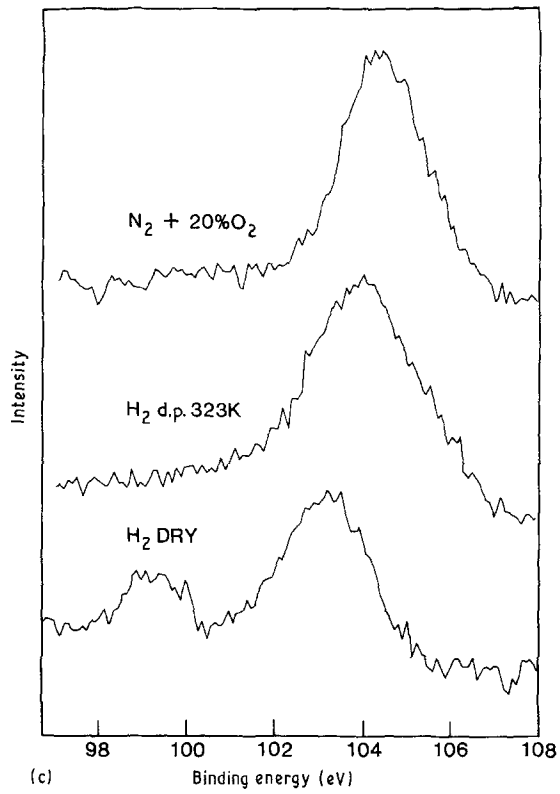

Figure 3 (a) Fe 2p (b) B 1s and (c) Si 2p ESCA spectra, from $Fe_{78.5}B_{13}Si_{8.5}$ amorphous alloy annealed at 673 K for 3.6 ksec in various annealing atmospheres.

zone formed during annealing at 623 K is extremely small and then the decrease of boron concentration in this zone is not so great.

These boron-depletion zones at the surface of the Fe–B–Si amorphous alloy ribbon should be formed in the case where the formation rate of a B_2O_3 film on a ribbon surface is higher than the diffusion rate of boron from the ribbon inside to surface [6]. Therefore, the formation of a boron-depletion zone is suppressed by lower formation rate of a B_2O_3 film on the alloy surface, or by higher diffusion rate of boron in the amorphous alloy [7]. The thickness of the boron-depletion zone formed during annealing at 623 K is smaller than that at higher temperatures, as shown in Fig. 5. This may be because of the lower formation rate of a B_2O_3 film due to the decrease of the reaction temperature.

3.3. Surface crystallization

Fig. 6 shows X-ray diffraction patterns from Fe–B–Si amorphous alloy ribbons annealed at 673 K for 3.6 ksec in various annealing atmospheres. Only halo patterns were observed on the amorphous alloy ribbons

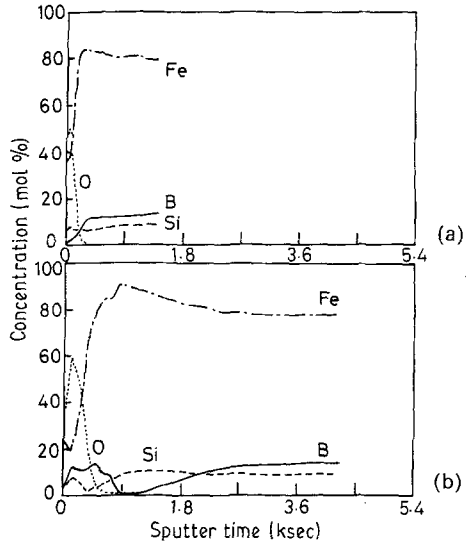

Figure 4 Depth profiles of iron, boron, silicon and oxygen at the surface of $Fe_{78.5}B_{13}Si_{8.5}$ amorphous alloys annealed at 673 K for 3.6 ksec in (a) dry hydrogen, and (b) hydrogen with a dew point of 323 K.

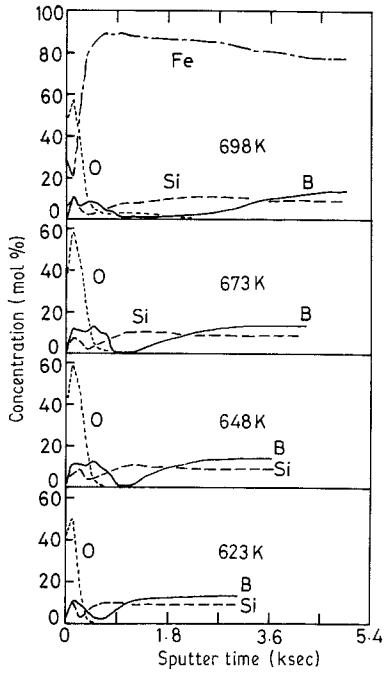

Figure 5 Change in depth profiles of iron, boron, silicon and oxygen at the surface of $Fe_{78.5}B_{13}Si_{8.5}$ amorphous alloy annealed for 3.6 ksec in hydrogen with a dew point of 323 K, upon annealing at various temperatures.

annealed in nitrogen, dry hydrogen, and N_2 + 20% O_2 atmospheres.

The X-ray diffraction pattern from the amorphous alloy annealed in a hydrogen atmosphere with a dew point of 323 K indicates the formation of an α-Fe crystalline phase in addition to the halo pattern. This crystallization is considered to take place at the surface of the Fe–B–Si amorphous alloy ribbon, because the α-Fe diffraction peak disappears on chemical polishing to remove about 0.5 μm of the ribbon surface.

The presence of α-Fe formed by this surface crystallization was also confirmed by means of conversion-

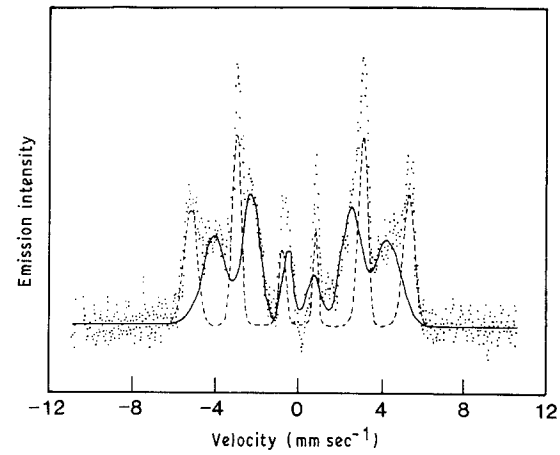

Figure 7 Conversion-electron Mössbauer spectrum from $Fe_{78.5}B_{13}Si_{8.5}$ amorphous alloy annealed at 673 K for 21.6 ksec in hydrogen with a dew point of 323 K.

electron Mössbauer spectroscopy, as shown in the six dotted-line peaks of Fig. 7.

Fig. 8 shows the influence of annealing temperature on X-ray diffraction patterns from Fe–B–Si amorphous alloy ribbon annealed in a hydrogen atmosphere with a dew point of 323 K. The intensity of the α-Fe(1 1 0) diffraction peaks decreases with decreasing annealing temperature, and no diffraction peaks of α-Fe were detected from the amorphous ribbon annealed at 623 K for 3.6 ksec. These results indicate that the crystallization temperature of the surface layer of Fe–B–Si amorphous alloy ribbon annealed in a wet hydrogen atmosphere is lower than 648 K.

On the contrary, when the amorphous ribbon was annealed in a dry hydrogen atmosphere no diffraction peaks of a crystalline phase were detected, even after annealing at 698 K for 3.6 ksec.

The reason why surface crystallization takes place during annealing in a wet hydrogen atmosphere,

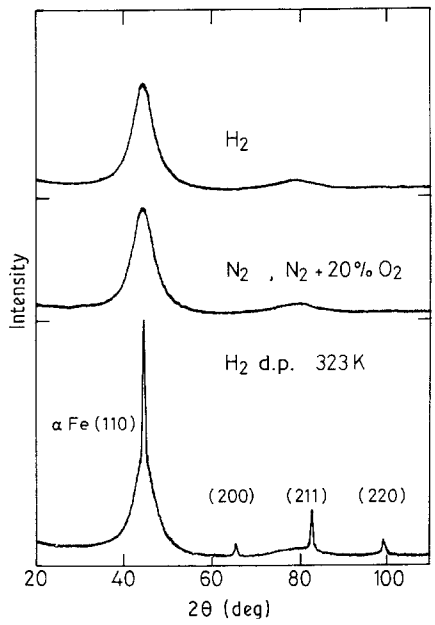

Figure 6 X-ray diffraction patterns from $Fe_{78.5}B_{13}Si_{8.5}$ amorphous alloy annealed at 673 K for 3.6 ksec in various annealing atmospheres.

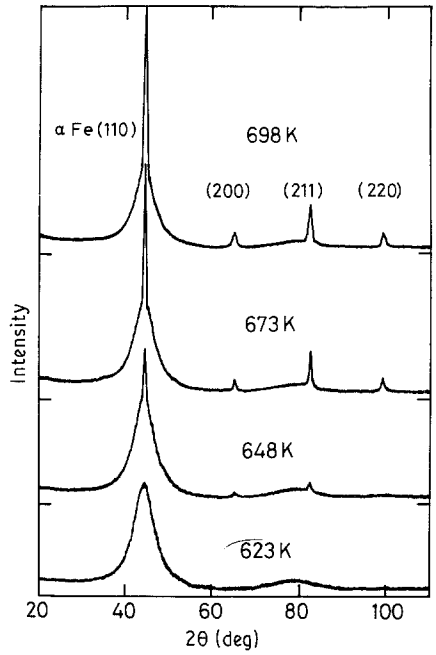

Figure 8 Change in X-ray diffraction patterns from $Fe_{78.5}B_{13}Si_{8.5}$ amorphous alloy annealed for 3.6 ksec in hydrogen with a dew point of 323 K upon annealing at various temperatures.

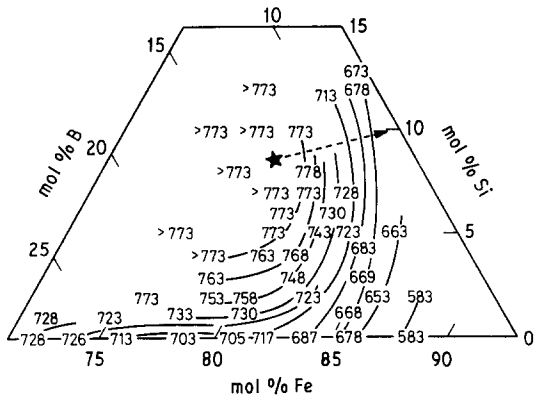

Figure 9 Composition dependence of crystallization temperature (K) in the Fe–B–Si alloy system after scanning at 0.33 K sec^{-1} (20 K min^{-1}). (after [8]) (★, →) See text.

although the annealing temperature is considerably lower than the crystallization temperature of the Fe–B–Si amorphous alloy used here, will now be discussed. The composition dependence of the crystallization temperature of the Fe–B–Si amorphous alloy system, Fig. 9, has been reported by Luborsky *et al.* [8], who indicated that the crystallization temperature of $Fe_{78.5}B_{13}Si_{8.5}$ (★) amorphous alloy decreases markedly with decreasing boron concentration in the alloy, but is not related to decreasing silicon concentration.

As described above, the alloy composition in the boron-depletion zone formed during annealing in a wet hydrogen atmosphere is 0 to 3 mol % B and 9 to 11 mol % Si (arrow). Therefore, the boron-depletion zone has an extremely low crystallization temperature and is crystallized easily upon annealing at about 673 K. The formation of a B_2O_3 surface film due to the selective oxidation of boron in wet hydrogen causes the formation of a boron-depletion zone with a low crystallization temperature beneath the surface oxide layer, and leads to surface crystallization during annealing. As shown in Fig. 8, the amount of α-Fe crystalline phase formed during annealing in wet hydrogen increases with increasing annealing temperature. This tendency corresponds well with annealing temperature dependence of the thicknesses of the boron-depletion zones (Fig. 5).

3.4. Magnetic properties

The iron loss, $W_{13/50}$, at 1.3 T and 50 Hz, and the magnetic flux density, B_1, at 100 A m^{-1}, of Fe–B–Si amorphous alloys annealed in various atmospheres at 673 K for 3.6 ksec are shown in Fig. 10. The iron loss improves to reach about 0.10 W kg^{-1} with annealing in argon, nitrogen, dry hydrogen and N_2 + 20% O_2, but annealing in hydrogen with a dew point of 323 K results in increased iron loss compared with the other atmospheres. The magnetic flux density, B_1, increases sharply with annealing at 673 K, but this improvement is independent of the atmospheres used.

The annealing temperature dependence of magnetic properties is shown in Fig. 11. On annealing in nitrogen and dry hydrogen, the minimum value of the iron loss, $W_{13/50}$, is obtained upon annealing at 648 to 673 K. The iron loss after annealing at 623 K is independent of the

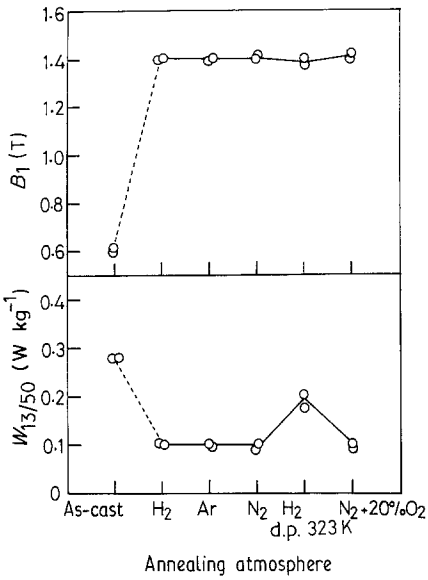

Figure 10 Change in magnetic properties of $Fe_{78.5}B_{13}Si_{8.5}$ amorphous alloy annealed at 673 K for 3.6 ksec in various annealing atmospheres.

annealing atmospheres used. Annealing of the Fe–B–Si amorphous alloy ribbon in a wet hydrogen atmosphere makes the iron loss $W_{13/50}$ almost constant or approximately 0.25 W kg^{-1} over the temperature range 623 to 698 K. The iron loss after annealing in wet hydrogen at 648 to 673 K is obviously worse than that in the other atmospheres.

When the Fe–B–Si amorphous alloy ribbons annealed in wet hydrogen at 648 to 673 K are chemically polished to remove about 1 μm of the ribbon surface, the iron loss is found to recover to the level obtained by annealing in a dry hydrogen atmosphere, as shown in Fig. 12.

3.5. Magnetic anisotropy

Annealing in a wet hydrogen atmosphere deteriorated the magnetic properties, especially the iron loss of Fe–B–Si amorphous alloy ribbon. Fig. 13 shows

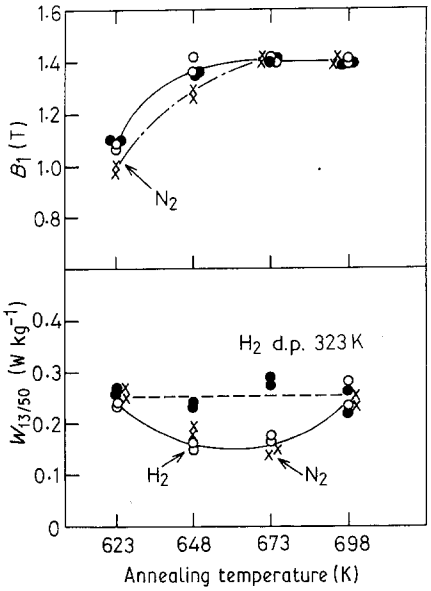

Figure 11 Annealing temperature dependence of magnetic properties of $Fe_{78.5}B_{13}Si_{8.5}$ amorphous alloys annealed for 3.6 ksec in dry hydrogen, dry nitrogen and hydrogen atmospheres with a dew point of 323 K.

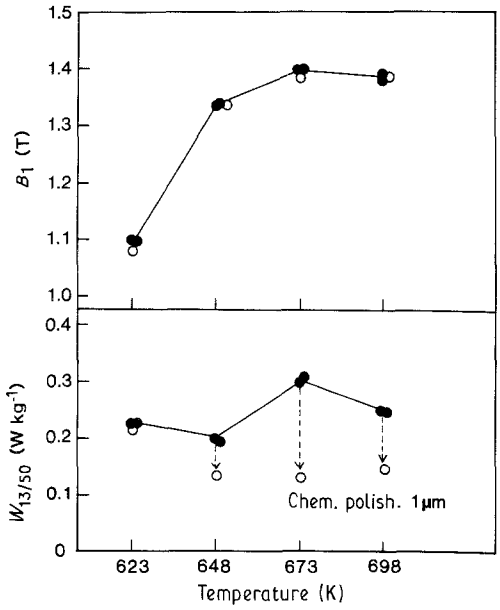

Figure 12 Change of magnetic properties by chemical polishing of $Fe_{78.5}B_{13}Si_{8.5}$ amorphous alloy annealed for 3.6 ksec in hydrogen with a dew point of 323 K.

transmission Mössbauer spectra of Fe–B–Si amorphous alloy ribbons annealed at 673 K in wet hydrogen and in vacuum under a magnetic field. No α-Fe crystalline phases, which have been detected by conversion electron Mössbauer spectroscopy (Fig. 7) and X-ray diffraction (Fig. 6), could be observed in the transmission spectra because of the difference in the relative detectable areas. The numerical values in Fig. 13 are the ratio $A_{2,5}/A_{1,6}$, where $A_{n,m}$ is the average area of the nth and the mth peaks of Mössbauer spectra. The direction of the magnetic moment is evaluated from the following equation [9]

$$\langle\theta\rangle = 90 - \sin^{-1}\{[3/2(A_{2,5}/A_{1,6})]/[1 + 3/4(A_{2,5}/A_{1,6})]\}^{1/2} \quad (1)$$

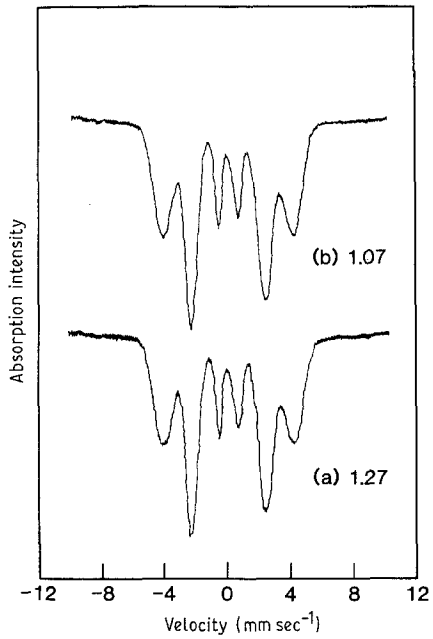

Figure 13 Mössbauer spectra from $Fe_{78.5}B_{13}Si_{8.5}$ amorphous alloy annealed at 673 K for 3.6 ksec in vacuum under (a) a magnetic field and (b) in hydrogen with a dew point of 323 K.

where $\langle\theta\rangle$ is the angle between the γ-ray and the direction of the magnetic hyperfine field.

The amorphous alloy ribbon annealed in vacuum under a magnetic field has an $A_{2,5}/A_{1,6}$ ratio of 1.27, indicating the development of an anisotropy with an easy direction almost parallel to the ribbon plane. Annealing in wet hydrogen decreases the $A_{2,5}/A_{1,6}$ ratio to 1.07 and slightly randomizes the direction of the magnetic moment.

3.6. Residual stresses in the surface crystalline layer

Magnetic properties of Fe–B–Si amorphous alloy ribbons with a high magnetostriction [10, 11] are expected to change through the generation of internal stress in the ribbon surface layer due to the density change with surface crystallization.

Fig. 14 shows the α-Fe (200) peak positions (2θ) plotted against $\sin^2\phi$, in the sample annealed in a wet hydrogen atmosphere. The positive gradient indicates the presence of a compressive stress in the surface crystalline layer formed during annealing. It is found that the gradient $d(2\theta)/d(\sin^2\phi)$ decreases and the compressive stress in the surface crystalline layer disappears on successively polishing the annealed sample surface with dilute HCl aqueous solution. This surface polishing has been previously confirmed by FT-IR and XRD to remove surface oxides only and not to damage the surface α-Fe crystalline layer.

This generation of compressive stress in the surface crystalline layer does not correspond with the expectation from the formation of the higher-density crystalline surface.

3.7. Deterioration of iron loss due to surface crystallization

Ok and Morrish [2] and Herzer and Hilzinger [12, 13] suggested, with regard to the surface crystallization of iron-based amorphous alloys, that the formation of the higher-density crystalline surface generates biaxial compressive stress in the amorphous bulk and tensile stress within the crystallized layer itself, and that this leads to an out-of-plane anisotropy in the bulk owing to positive magnetostriction.

This mechanism explains the present experimental

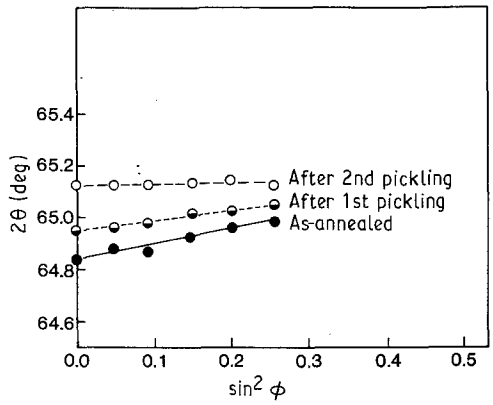

Figure 14 Relationship between the positions of the α-Fe(200) diffraction peak and $\sin^2\phi$, in $Fe_{78.5}B_{13}Si_{8.5}$ amorphous alloys annealed at 673 K for 3.6 ksec in hydrogen with a dew point of 323 K, and subsequently polished with dilute HCl aqueous solution.

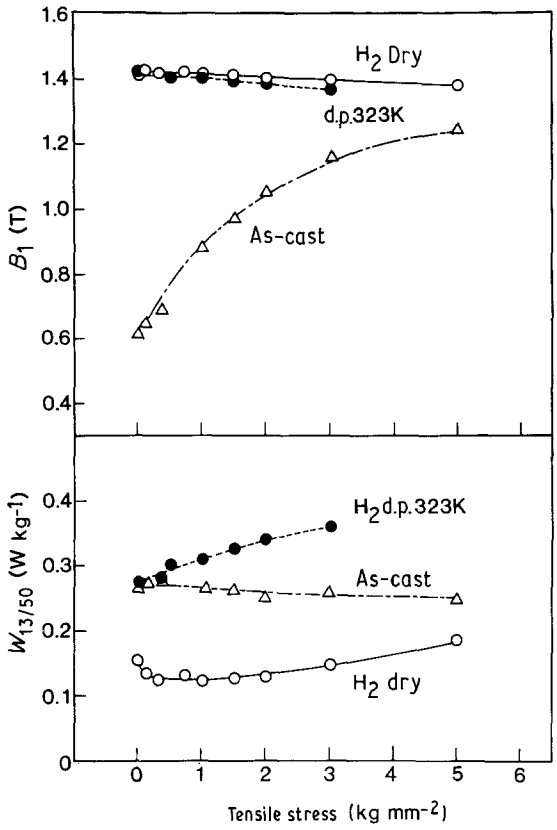

Figure 15 Tensile stress dependence of magnetic properties of $Fe_{78.5}B_{13}Si_{8.5}$ amorphous ribbons as cast and annealed in dry hydrogen, and in hydrogen with a dew point of 323 K.

results regarding the changes in iron loss and magnetic anisotropy determined by Mössbauer spectra. However, the presence of compressive stress was detected by X-ray diffraction in the surface crystalline layer of Fe–B–Si ribbons annealed in wet hydrogen, as shown in Fig. 14. If the uniform compressive stress was present in the crystalline surface layer, an internal tensile stress would be generated in the amorphous bulk and lead to an in-plane anisotropy owing to positive magnetostriction, and the iron loss would improve. These expectations do not agree with the present experimental results. Therefore, the distribution of compressive stress in the surface crystalline layer is not considered to be uniform.

Fig. 15 shows the tensile stress dependence of magnetic properties of the amorphous alloy ribbons annealed in dry and wet hydrogen atmospheres. The iron loss, $W_{13/50}$ and the magnetic flux density, B_1, of the amorphous ribbon annealed in dry hydrogen show only small changes even upon applying a tensile stress [14]. But the iron loss of the amorphous ribbon with a surface crystalline layer formed during annealing in wet hydrogen increases with increased tensile stress. If the surface crystalline layer generated a compressive stress field with the uniform distribution in the amorphous bulk, the tensile stress applied from outside would compensate the compressive stress and result in a decreasing iron loss.

The present experimental results indicate that the surface crystalline layer induced by selective oxidation of boron generates an irregular distribution of the stress field in the amorphous bulk. This may be due to the non-uniformity of the stress distribution in the

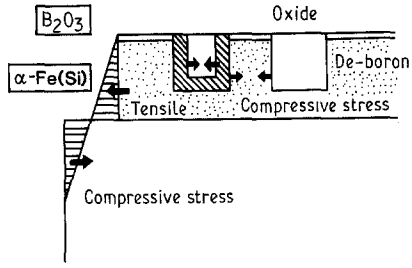

Figure 16 A schematic model of stress distribution in the surface layer of $Fe_{78.5}B_{13}Si_{8.5}$ amorphous alloy annealed in a wet hydrogen atmosphere.

surface crystalline layer that results following the non-uniformity of the thickness of the oxide film on the surface crystalline layer, as shown in Fig. 16.

4. Conclusion

Annealing of an Fe–B–Si amorphous alloy ribbon in an $H_2 + H_2O$ atmosphere resulted in the formation of a boron-depletion zone with an alloy composition of 0 to 3 mol % B and 9 to 11 mol % Si under an oxide film. The alloy in this depletion zone crystallized into α-Fe during annealing even at a temperature below the crystallization temperature, including an out-of-plane magnetic anisotropy in the amorphous alloy ribbon and causing deterioration of the iron loss.

On the other hand, annealing in nitrogen, argon, hydrogen and air resulted in neither the formation of a boron-depletion zone nor surface crystallization.

References

1. Y. KITANO, C. MAEDA, M. SHIMIZU, S. KOBAYASHI and N. MORITO, *J. Jpn Inst. Metals* **53** (1989) 258.
2. H. N. OK and A. H. MORRISH, *Phys. Rev. B* **23** (1981) 2257.
3. M. ACKERMANN, H. G. WAGNER, U. GONSER and P. STEINER, *Hyperfine Interactions* **27** (1986) 397.
4. H. G. WAGNER, M. ACKERMANN, R. GAA and U. GONSER, in "Proceedings of the 5th International Conference on Rapidly Quenched Metals", edited by S. Steeb and H. Warlimont (North-Holland, Amsterdam, 1985) p. 247.
5. U. KOSTER, *Mater. Sci. Engng.* **97** (1988) 233.
6. P. KOFSTAD, "High-Temperature Oxidation of Metals" (Wiley, New York, 1966) p. 269.
7. C. F. CHANG and J. MARTI, *J. Mater. Sci.* **18** (1983) 2297.
8. F. E. LUBORSKY, J. J. BECKER, J. L. WALTER and H. H. LIEBERMAN, *IEEE Trans. Mag.* **MAG-15** (1979) 1146.
9. N. SAEGUSA and A. H. MORRISH, *J. Magn. Magn. Mater.* **31** (1983) 1555.
10. S. ITO, K. ASO, Y. MAKINO and S. UEDAIRA, *Appl. Phys. Lett.* **37** (1980) 665.
11. A. DATTA, D. NATHASINGH, R. J. MARTIS, P. J. FLANDERS and C. D. GRAHAM Jr, *J. Appl. Phys.* **55** (1984) 1784.
12. G. HERZER and H. R. HILZINGER, *J. Magn. Magn. Mater.* **62** (1986) 143.
13. H. R. HILZINGER and G. HERZER, *Mater. Sci. Engng.* **99** (1988) 101.
14. T. SASAKI, E. SHIMOMURA and K. YAMADA, *IEEE Trans. Magn.* **MAG-23** (1987) 3587.

Received 13 July
and accepted 22 November 1989